Journal Name

COMMUNICATION

Multicolour photochromic fluorescence of a fluorophore encapsulated in a metal–organic framework

Received 00th January 20xx,
Accepted 00th January 20xx

DOI: 10.1039/x0xx00000x

www.rsc.org/

Kenji Hirai,*[abc] Taisei Kitagawa,[b] Hideki Fujiwara,[d] Jenny Pirillo,[e] Yuh Hijikata,[e] Tomoko Inose,[ab] Hiroshi Uji-i[abf]

A fluorophore encapsulated in a metal–organic framework showed photochromic multicolour fluorescence. Irradiation with a ultraviolet laser induced relocation of the fluorophore from polar to nonpolar environment, altering the emission from red to blue. This change in emission color can be repeatably recovered by heating the fluorophore–MOF composite.

Photochromism is a reversible colour change under light irradiation, and is important in the development of optical memory,[1] photoswitches,[2] and super-resolution fluorescent imaging.[3] The photochromic materials have been fabricated by embedding photochromic moieties into molecular assemblies.[4] Metal–organic frameworks (MOFs),[5–8] composed of metal ions and organic ligands, are excellent platforms into which photochromic moieties can be introduced. To date, photochromism in MOFs has been predominantly limited to switching between two reversible states, such as the structural transformation of photochromic moieties,[9–13] the reversible redox reaction of organic ligands,[14–19] photodimerization of guest molecules,[20] or spin transitions between d-orbitals.[21] Despite the promising applications of multimode switching materials, multistate photochromism in MOF has not been realized yet.

One of approaches to designing multicolour photochromism is encapsulating multicolour fluorophores in porous solids such as MOFs.[22, 23] Fluorophores based on twisting intramolecular charge transfer (TICT)[22-24] exhibit multicolour fluorescence depending on the environment polarity.[24–27] The fluorescent wavelength of TICT fluorophores in porous solids varies with site-specific polarity.[27] Thus, the change in fluorescent wavelength can be triggered by relocation of the TICT fluorophores in the pores. These considerations inspired us to look into the possibility to fabricate multicolour photochromic materials by introducing the TICT fluorophores into MOFs. This idea relies on the hypothesis that the TICT fluorophores are relocated in the pores of MOFs under light irradiation. The light irradiation on TICT fluorophores induces the charge transfer through twisting of the donor part against the acceptor part.[19] The twisting with charge separation state would allow the dynamic motion associated with electrostatic repulsion, leading to relocation of TICT fluorophores within the pores of MOFs. Consequently, the fluorescent colour could be altered by the light irradiation on MOFs accommodating TICT fluorophores.

Three-dimensional MOF $[Zn_2(bdc)_2(dabco)]_n$ (**1**)[28] is an excellent platform for accommodating TICT fluorophores (bdc, 1,4-benzenedicarboxylate; dabco, 1,4-diazabicyclo[2.2.2]octane). The oxygen atoms in carboxylates coordinated to zinc ions called paddle wheel unit generally provide polar sites for the guest molecules.[29] in addition to this, other moieties in the pores, such as the sp^3 carbon of dabco, provide nonpolar sites for guest molecules. The pores of **1** provide the TICT fluorophores with various polar sites, leading to site-dependent fluorescence. Herein, we aimed to fabricate multicolour photochromic materials by encapsulating TICT fluorophores in MOFs.

[a] *Division of Photonics and Optical Science, Research Institute for Electronic Science (RIES), Hokkaido University, North 20 West 10, Kita ward, Sapporo, Hokkaido, Japan. E-mail: hirai@es.hokudai.ac.jp*
[b] *Division of Information Science and Technology, Graduate School of Information Science and Technology, Hokkaido University, North 14 West 9, Kita ward, Sapporo, Hokkaido, Japan.*
[c] *Precursory Research for Embryonic Science and Technology (PRESTO), Japan Science and Technology Agency (JST), 4-1-8 Honcho, Kawaguchi, Saitama, Japan.*
[d] *Department of Electronics and Information Engineering, Faculty of Engineering, Hokkai-Gakuen University, 1-1, South 26 West 11, Chuo ward, Sapporo, Hokkaido, Japan.*
[e] *Institute for Chemical Reaction Design and Discovery (WPI-ICReDD), Hokkaido University, Sapporo, Hokkaido, Japan.*
[f] *Department of Chemistry, Katholieke Universiteit Leuven, 200F, 3001 Heverlee, Leuven, Belgium.*

†Electronic Supplementary Information (ESI) available: details of experiments and theoretical calculation, SEM, XRD, ^{1}H-NMR, UV-vis absorption and photoluminescent spectroscopy. See DOI: 10.1039/x0xx00000x

To demonstrate the proof of concept, we synthesized crystals of **1** of several tens of micrometres in size using a solvothermal method (**Figs. S1–S2**). The solvent molecules in crystals of **1** were removed under vacuum at 120 °C. After activating **1**, DMASP was introduced into its pores through sublimation at 220 °C (DMASP, 4-[4-(dimethylamino)styryl]pyridine). The main XRD peaks of **1** accommodating DMASP (**1**⊃DMASP) corresponds to as-synthesized **1.** Furthermore, no DMASP XRD peaks were observed in the pattern of **1**⊃DMASP**.** These results indicate that DMASP was successfully introduced into **1** with retention of the framework structures. (**Fig. S2**). The ratio of DMASP/H_2bdc/dabco was estimated to be 1:8:4 by ^{1}H-NMR (**Fig. S3a**). The number of DMASP molecules in a single unit cell of **1** was calculated to be 0.25. The length along the *c*-axis of **1** was 0.9 nm. In contrast, the length of DMASP was approximately 2 nm, which is longer that the unit cell of **1** (approximately 1 nm). This can be the reason why the number of DMASP molecules was less than the number of unit cells of **1**.

DMASP can show two emission pathways by the excitation using an ultraviolet light. One is the direct emission from the local excited state, which is observed from 380 to 420 nm. The other is the emission from TICT state, where the dimethylamino group was twisted with respect to styrylpyridine, followed by charge transfer from the dimethylamino group to styrylpyridine. In general, the emission from TICT state is dominant in the polar environments. The emission wavelength from the TICT state is dependent on stabilization of the TICT state by the polar medium. Increasing the polarity of the medium shifted the emission to a longer wavelength[24] (**Fig. S4**). **1**⊃DMASP showed emission with a peak maximum at 600 nm (**Figs. 1b, 1e and S5**).

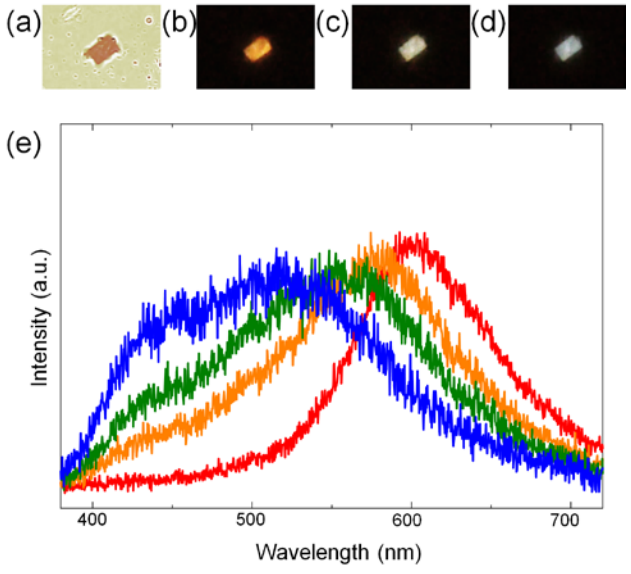

Fig. 1. (a) Microscopic image of **1**⊃DMASP. (b–d) Fluorescent images of **1**⊃DMASP under pulsed laser irradiation. Time passes from left to right. (e) Fluorescent spectra of **1**⊃DMASP after various pulsed laser exposure times at 355 nm: 0 s (red), 30 s (orange), 60 s (green), and 150 s (blue).

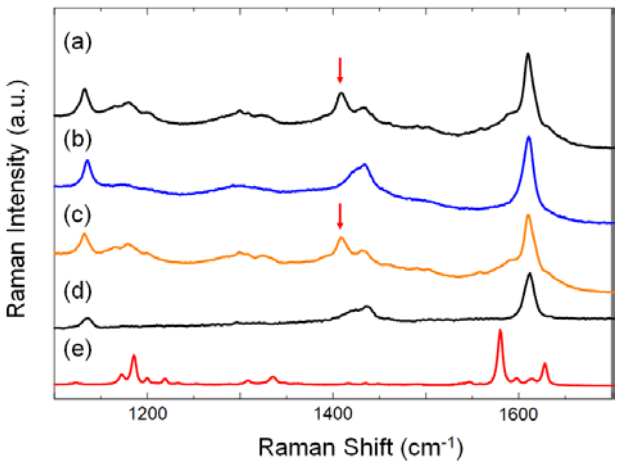

Fig. 2. Raman spectra of (a) **1**⊃DMASP after pulsed laser irradiation and heating, (b) **1**⊃DMASP after pulsed laser irradiation, (c) **1**⊃DMASP, (d) **1**, and (e) DMASP. Red arrow indicates the peak due to the interaction between carboxylate and DMASP.

As the emission of DMASP from the local excited state was observed at 390–420 nm, **1**⊃DMASP emission at 600 nm was assigned as the emission from the TICT state, meaning that the TICT state was stabilized by the polar environment inside the pores of **1**. The interaction between the carboxylate groups of bdc and DMASP was observed by microscopic Raman spectroscopy (**Fig. 2c-e**). The symmetric vibration of the carboxylate groups was shifted to a lower wavenumber, indicating electrostatic interaction between carboxylate and DMASP. This interaction provided DMASP with the polar environment, leading to the emission from the TICT state.

Through excitation using a pulsed laser of 355 nm, the fluorescence colour of **1**⊃DMASP was gradually changed from orange to blue (**Fig. 1a-d** and supporting movie). The emission of **1**⊃DMASP was shifted from 600 to 430 nm with continuous irradiation with the pulsed laser (**Fig. 1e**). The intensity differences at each wavelength (600, 550, 500, and 450 nm) were plotted against the pulsed laser exposure time (**Fig. S6**). The intensity at 600 nm rapidly decreased, reaching a plateau at around 150 s. The intensity at 550 nm initially increased, but then decreased after 50 s. In contrast to the chronological change at 600 nm, the intensities at 450 and 500 nm continuously increased until 150 s. Once the emission wavelength was shifted from 600 to 430 nm, the laser irradiation does not induce further change of the emission wavelength. It is noted that the emission wavelength of **1**⊃DMASP remained same after the end of the laser irradiation (Fig. S7). In other word, it is possible to isolate each colour by stopping laser irradiation. Additionally, the opposite change of emission wavelength, i.e. from 430 to 600 nm, does not occur by laser irradiation.

The environmental change of DMASP under the laser irradiation was evidenced by microscopic Raman spectroscopy of **1**⊃DMASP. The symmetric vibration of the carboxylate group in **1**⊃DMASP after laser irradiation resembled that of **1** without

guest molecules (**Fig. 2b**), suggesting no significant interaction between DMASP and carboxylate groups. This result indicated the relocation of DMASP from polar carboxylate sites to weakly polar sites.

The pulsed laser could allow multiphoton absorption in the **1**⊃DMASP, triggering the relocation of DMASP in the pores. However, the increase of emission intensity at 400-500 nm was also observed under continuous wave (CW) laser irradiation 375 nm, as shown in **Fig. S8a**. This result indicated that the excitation of DMASP, namely, single photon absorption by DMASP, induced DMASP relocation. In order to clarify the effect of amount of DMASP, the amount of DMASP in **1** was reduced by reducing the amount of DMASP used in sublimation process. The molar ratio of DMASP in **1** was reduced from 0.25 molecules to 0.12 molecules per single unit cell of **1**, which was confirmed by ^{1}H-NMR (Fig. S3b). 1 accommodating reduced amount of DMASP is denoted as **1**⊃DMASP$_{half}$. The emission wavelength of **1**⊃DMASP$_{half}$ under the irradiation of CW laser shifted faster than **1**⊃DMASP (Fig. S8b). This result indicated that the larger amount of DMASP requires more photons to induce the shift of emission wavelength, but the overall phenomena of emission colour change do not depend on the amount of DMASP.

In order to unveil the mechanism in relocation of DMASP, theoretical calculations of **1**⊃DMASP were carried out. Prior to the optimization of DMASP in **1**, the framework geometry of **1** was optimized by using density-functional tight-binding (DFTB) method[30] under periodic boundary condition. We referred to the reported crystal structure of **1**,[28] and all atomic positions of **1** were optimized step by step. As shown in **Fig. 3**, three

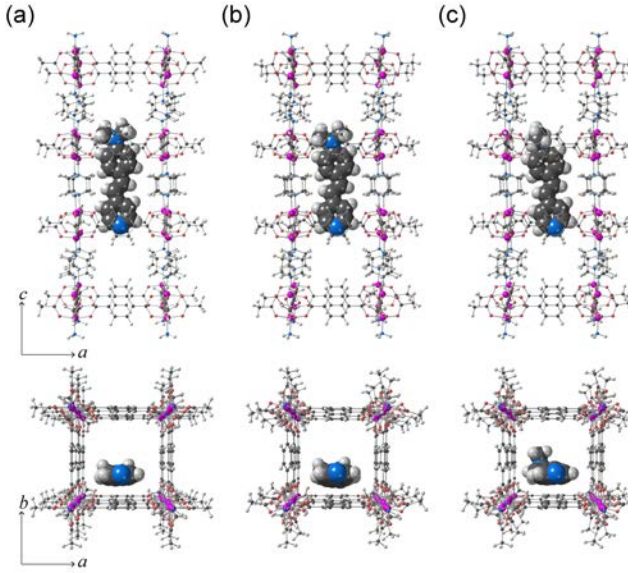

Fig. 3. Optimized model structures of **1**⊃DMASP: (a) DMASP without twisting at the ground state, (b) DMASP without twisting at the excited state, and (c) DMASP with twisting at the excited state. Grey, white, red and blue spheres indicate carbon, hydrogen, oxygen and nitrogen atoms, respectively.

sequential pores in the optimized framework were utilized for following calculations. In order to reduce the calculation cost, the atomic positions of **1** was fixed when optimizing the conformation of DMASP in **1**. The spatial position of DMASP in **1** was simulated by geometry optimization of DMASP with quantum mechanical and **1** with molecular mechanics calculations using the ONIOM algorithm.[31, 32] The geometries of DMASP at ground and excited states without twisting motion were simulated (**Figs 3a-b**). The spatial location of DMASP at the excited state was similar to the ground state. However, the simulation of DMASP with twisting motion at the excited states showed different arrangement of DMASP in the pore. When the dimethyl amino group of DMASP was rotated at 90 degree, styrylpyridine moiety of DMASP was strained and dimethyl amino group located closer to oxygen of carboxylate group due to charge transfer from the amino group to styrylpyridine moiety,[24] which changes the dimethyl amino group more positive and the dimethyl amino group interact with zinc cluster closer (**Figs 3c**). The distance between the closest oxygen in carboxylate and hydrogen in the methyl group were 2.910 Å and 2.703 Å at the ground and excited states, respectively. The polar environment around zinc cluster tends to induce the twisting of dimethyl amino group at the excited state, resulting the charge transfer and movement of DMASP. When DMASP returned to the ground state with twisting again, the repulsive interaction between the dimethyl amino group and zinc cluster could induce additional movement. DMASP is dynamic in the pore and allowed to relocate in non-polar area. This dynamics of DMASP in **1** can explain the reason why DMASP is relocated in the pore by laser irradiation.

Despite the one-way change in fluorescent wavelength under laser irradiation, the fluorescence wavelength of **1**⊃DMASP can be recovered to the original red fluorescence upon heating (**Fig. S9**). Indeed, the characteristic carboxylate peak appeared again in the Raman spectrum after heating, indicating that heating allowed DMASP to return to the original polar sites of **1** (**Fig. 2a**), which could be thermodynamically the most stable sites in the pores.

In summary, we have demonstrated the multicolour photochromic fluorescence of a fluorophore–MOF composite through laser irradiation. DMASP, a fluorophore with emission from TICT states, was encapsulated in a MOF and interacted with polar carboxylate sites, resulting in fluorescence at around 600 nm. Under UV laser irradiation, DMASP was relocated from polar to nonpolar sites, resulting in a fluorescence wavelength shifts from 600 to 400 nm. DFT calculations demonstrated that photoexcitation of DMASP could induces the additional dynamic motion to relocate itself in the pores. By heating the fluorophore–MOF composite, DMASP moved back to the original polar state, showing fluorescence at 600 nm. This represents the first example of a MOF–fluorophore composite showing multicolour photochromic fluorescence. The multicolour photochromism of MOFs will realize the generation of mass optical memory, multimode switching materials, and multicolour imaging technologies.

Acknowledgments

This work was supported by funding from JSPS KAKENHI (Grant Nos. JP18H01948, JP18K19085) and JST PRESTO (JPMJPR18TA) to K.H. This work was partially supported by funding from JSPS

KAKENHI (Grant Nos. JP17K05016, JP19H04529, JP18H03882, JP17H03003) and the Nippon Sheet Glass Foundation for Materials Science and Engineering to H.F. The work by J. P. and Y.H. is partially supported by JSPS Scientific Research on Innovative Areas, Coordination Asymmetry (19H04570).

Notes and references

1 M. Irie, *Chem. Rev.* 2000, **100**, 1683–1684.

2 M. Irie, T. Fukaminato, K. Matsuda, S. Kobatake, *Chem. Rev.* 2014, **114**, 12174–12277.

3 Y. Arai, S. Ito, H. Fujita, Y. Yoneda, T. Kaji, S. Takei, R. Kashihara, M. Morimoto, M. Irie, H. Miyasaka, *Chem. Commun.*, 2017, **53**, 4066-4069

4 L. Wang and Q. Li, *Chem. Soc. Rev.*, 2018, **47**, 1044-1097.

5 S. Kitagawa, R. Kitaura and S. I. Noro, *Angew. Chemie - Int. Ed.*, 2004, **43**, 2334–2375.

6 H. Furukawa, K. E. Cordova, M. O'Keeffe and O. M. Yaghi, *Science*, 2013, **341**, 1230444.

7 Y. Inokuma, S. Yoshioka, J. Ariyoshi, T. Arai, Y. Hitora, K. Takada, S. Matsunaga, K. Rissanen and M. Fujita, *Nature*, 2013, **495**, 461–466.

8 K. Sumida, D. L. Rogow, J. A. Mason, T. M. McDonald, E. D. Bloch, Z. R. Herm, T. H. Bae and J. R. Long, *Chem. Rev.*, 2012, **112**, 724–781.

9 V. I. Nikolayenko, S. A. Herbert and L. J. Barbour, *Chem. Commun.*, 2017, **53**, 11142–11145.

10 F. Luo, C. Bin Fan, M. B. Luo, X. L. Wu, Y. Zhu, S. Z. Pu, W. Y. Xu and G. C. Guo, *Angew. Chem. Int. Ed.*, 2014, **53**, 9298–9301.

11 J. Park, D. Feng, S. Yuan and H. C. Zhou, *Angew. Chem. Int. Ed.*, 2015, **54**, 430–435.

12 J. Park, Q. Jiang, D. Feng and H. C. Zhou, *Angew. Chem. Int. Ed.*, 2016, **55**, 7188–7193.

13 Z. Li, G. Wang, Y. Ye, B. Li, H. Li, B. Chen, *Angew. Chem. Int. Ed.*, 2019, **58**, 18025 – 18031.

14 J. K. Sun, L. X. Cai, Y. J. Chen, Z. H. Li and J. Zhang, *Chem. Commun.*, 2011, **47**, 6870–6872.

15 J. K. Sun, P. Wang, Q. X. Yao, Y. J. Chen, Z. H. Li, Y. F. Zhang, L. M. Wu and J. Zhang, *J. Mater. Chem.*, 2012, **22**, 12212–12219.

16 Y. N. Gong and T. B. Lu, *Chem. Commun.*, 2013, **49**, 7711–7713.

17 A. Mallick, B. Garai, M. A. Addicoat, P. S. Petkov, T. Heine and R. Banerjee, *Chem. Sci.*, 2015, **6**, 1420–1425.

18 C. Chen, J. K. Sun, Y. J. Zhang, X. D. Yang and J. Zhang, *Angew. Chem. Int. Ed.*, 2017, **56**, 14458–14462.

19 H. Y. Li, Y. L. Wei, X. Y. Dong, S. Q. Zang and T. C. W. Mak, *Chem. Mater.*, 2015, **27**, 1327–1331.

20 M. Tu, H. Reinsch, S. Rodríguez-Hermida, R. Verbeke, T. Stassin, W. Egger, M. Dickmann, B. Dieu, J. Hofkens, I. F. J. Vankelecom, N. Stock, R. Ameloot, *Angew. Chem. Int. Ed.*, 2019, **58**, 2423 –2427.

21 N. F. Sciortino, K. R. Scherl-Gruenwald, G. Chastanet, G. J. Halder, K. W. Chapman, J. F. Létard and C. J. Kepert, *Angew. Chem. Int. Ed.*, 2012, **51**, 10154–10158.

22 B. Xu, Z. Gao, Y. Wei, Y. Liu, X. Sun, W. Zhang, X. Wang, Z. Wanga, X. Meng, *Nanoscale*, 2020, **12**, 4833–4838.

23 Y. Wei, H. Dong, C. Wei, W. Zhang, Y. Yan, Y. S. Zhao, *Adv. Mater.*, 2016, **28**, 7424–7429.

24 M. Sowmiya, A. K. Tiwari, Sonu and S. K. Saha, *J. Photochem. Photobiol. A Chem.*, 2011, **218**, 76–86.

25 N. A. Garcia and T. Kowalczyk, *J. Phys. Chem. C*, 2017, **121**, 20673–20679.

26 Z. B. Sun, S. Y. Li, Z. Q. Liu and C. H. Zhao, *Chinese Chem. Lett.*, 2016, **27**, 1131–1138.

27 N. Nakashima, and D. Phillips, *Chem. Phys. Lett.*, 1983, **97**, 337–341.

28 D. N. Dybtsev, H. Chun and K. Kim, *Angew. Chem. Int. Ed.*, 2004, **43**, 5033–5036.

29 J. L. C. Rowsell, E. C. Spencer, J. Eckert, J. A. K. Howard, and O. M. Yaghi, *Science* 2013, **309**, 1350–1355.

30 M. Gaus, Q. Cui, and M. Elstner, *J. Chem. Theory Comput.* 2011, **7**, 931-948.

31 S. Dapprich, I. Komaromi, K. S. Byun, K. Morokuma, M. J. Frisch, *J. Mol. Struct.: THEOCHEM* 1999, **461**, 1−21.

32 T. Vreven, K. S. Byun, I. Komaromi, S. Dapprich, J. A. Montgomery, K. Morokuma, M. J. Frisch, *J. Chem. Theory Comput.* 2006, **2**, 815−826.

